32nd Electric Vehicle Symposium (EVS32)
Lyon, France, May 19 - 22, 2019

Optimal speed synchronization control with disturbance compensation for a hybrid dual-clutch transmission

Wei Huang[1], Jianlong Zhang[1], Jianfeng Huang[1], Chengliang Yin[1] and Lifang Wang[2]

[1]*School of Mechanical Engineering, Shanghai Jiao Tong University, Dongchuan Road 800, Shanghai, 200240, P.R. China. Email:huangwei1993223@sjtu.edu.cn*

[2]*Institute of Electrical Engineering, Chinese Academy of Sciences, Beijing, P.R. China.*

Summary

This paper presents a gear shift method for a hybrid dual clutch transmission (HDCT) with integrated electric motor in pure electric drive mode. Benefitting from the fast-dynamic response ability of the motor, the speed of the oncoming gear can be adjusted to that of the sleeve of the synchronizer, which implies a good shifting performance—shorter torque interruption interval and lower impact. The proposed speed synchronization controller combined model predictive control (MPC) with a time-domain disturbance observer, which can eliminate effects from unmodelled dynamics and exogenous disturbances. Simulation and experiment results demonstrate that the effectiveness of the proposed approach in attaining a rapid and robust speed synchronization performance. Furthermore, the method applied in this topology is also applicable to some other clutchless automatic manual transmission (CLAMT) powertrain in electric vehicle where the motor speed regulation is indispensable in gear shift process.

Keywords: powertrain, transmission, plug in hybrid electric vehicle, optimization, strategy

1 Introduction

Due to the features of simple structure, high efficiency and power-on gear shift ability, dual clutch transmission (DCT) has been widely used in the recent decade. Stricter environmental policies and fuel targets raise higher requirements to powertrain systems. Different hybrid dual clutch transmission systems (HDCTs) have been developed, where the electric motor can be attached to input shaft, countershaft or output shaft [1-3]. Fig. 1 is the schematic diagram of a Motor-Integrated 6-Speed DCT. Plug in hybrid electric vehicle equipped with HDCT will operate in a pure electric drive mode until the battery level drops to the threshold of charge-sustaining mode. Therefore, to realize a wider range of torque application and higher energy efficiencies than fixed gear ratio, gear change among odd gears is necessary. When the HDCT operates in pure electric drive mode, it can be seen as equivalent to a clutchless automatic manual transmission (CLAMT). Synchronizer becomes the primary shift element and the integrated motor can help to match the oncoming gear speed with the sleeve velocity of synchronizer.

A great deal of previous research of the CLAMT systems has focused on overcoming the impact of torque interrupt during gear change. Reference [4] introduced a CLAMT powertrain system used in battery electric bus, in which the clutch and synchronizer are both omitted. The paper points out that a small speed difference

between motor and output shaft is the precondition for a smooth shift, which can avoid “kick tooth” phenomenon. The gear shift process of CLAMT powertrain system is accomplished by the operations of gear release, gear select, speed synchronization, gear engagement and torque recover in order. The speed synchronization phase accounts for nearly 50% of the total shift time based on the experimental results [5]. Several control strategies have already been adopted to reduce the time of speed synchronization. Reference [1] used shifting duration, vibration dose value and vehicle longitudinal jerk as indicators to evaluate gear shift performance in a CLAMT system, and they employed a common proportional-integral-derivative (PID) type controller to enable closed-loop speed control for motor speed synchronization. To implement a precise motor speed regulation, a fixed-gain PID speed regulation controller is replaced by sliding-mode controller [6]. A control algorithm that combines speed and torque control of the AMT vehicle powertrain to achieve shifting control without using the clutch is presented in [7], where the combined control algorithm based on feed-forward, bang-bang and PID control can realize precise engine speed control. Overall, whether used in conventional vehicle or hybrid electric vehicle, these studies in CLAMT powertrain control highlight the predominant importance of a rapid and robust motor speed synchronization process. The gear shift process of the HDCT confronts some other challenges like big gear ratio difference between adjacent odd gears and large inertia to be synchronized. Moreover, the electric motor within the DCT is cooled by transmission lubricant. As a result, the motor torque may be disturbed by oil stirring resistance during gear change.

This paper presents a speed synchronization controller for the HDCT system shown in Fig.1. The benefit of this approach is that the combined control algorithm is robust to unknown disturbance since it can be suppress by incremental MPC and disturbance observer (DO). In addition, quantitative method to determine MPC tuning parameters is given in this paper. Section 2 analyzes the gear shift process of the HDCT in pure electric drive mode in details and built the powertrain lumped model, following the combined controller design method. In Section 4, the simulation and experiment results are presented. The fifth section provides a conclusion to this paper.

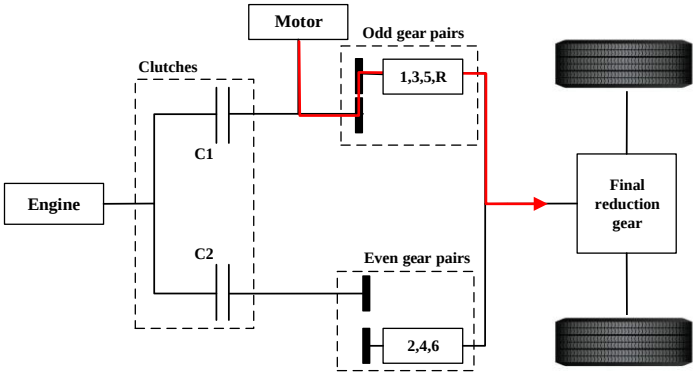

Figure 1: Layout of the HDCT and its pure electric drive mode

2 Problem formulation

2.1 Gear shift process in pure electric drive mode

Fig. 2 shows the gear shift flowchart of the HDCT in pure electric drive mode. This process can be subdivided into gear releasing phase, speed regulation phase, gear engagement phase and torque recover phase, and it mainly involved with the vehicle control unit (HCU), motor control unit (MCU) and transmission control unit (TCU), where the measurements and control signals among these controllers can be delivered through the controller area network (CAN) bus. HCU provides an overarching control of the hybrid powertrain system and coordinates work between the MCU and TCU in gear shift process. Based on gear shift schedule of the pure electric drive mode, HCU determines whether a gear change event is activated. To facilitate the release of synchronizer mechanism, MCU can control the motor to be de-energized.

During speed regulation phase, HCU calculates the target speed of the motor in real time and adjusts the motor speed according to proposed speed synchronization algorithm. The speed regulation phase will last until the difference between the actual speed and the target speed of the motor is within threshold. The specific value depends on mechanical characteristics of the gears and synchronizers, which can be obtained through

bench test [4]. After the motor speed is stabilized around the target speed for some time, the gear shift process can forward to gear engagement phase. TCU will actuate synchronizer to engage the oncoming gear, where synchronizer generates frictional force to reduce the synchronized side speed at upshift or increase the synchronized side speed at downshift. Because the motor speed is close to the target speed, the wear and tear of the synchronizer during engagement can be substantially reduced. In torque recover phase, MCU receives the torque-recovering command form HCU according to the power management strategy. This paper mainly concerns with how to reduce the speed regulation time while ensuring a smooth gear engagement process by suppressing the motor speed and torque fluctuation before engagement.

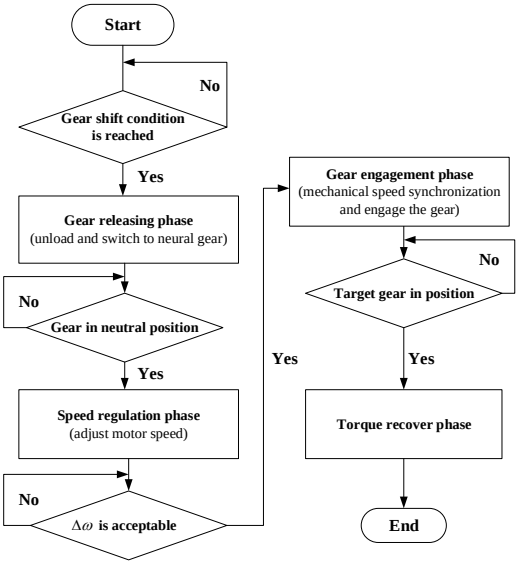

Figure 2: Gear shift process of the HDCT in pure electric drive mode

2.2 Powertrain lumped model

Since clutches and synchronizers are fully disengaged in speed regulation phase, the dynamic model of the HDCT powertrain system in EV mode can be degenerated into a 2-DOF model. The equations of motion of the system are as follows:

$$J_{e,m}\dot{\omega}_m = T_m - b_{e,m}\omega_m - T_f \tag{1}$$

$$J_v\dot{\omega}_v = -(Mgrsin\theta + \frac{1}{2}\rho_{air}AC_DV^2r + Mgfrcos\theta) \tag{2}$$

where ω_m and ω_v are the rotational speed of the motor and wheel, r is the radius of the tire, $J_{e,m}$ denotes the equivalent inertia converted to the motor output shaft, J_v is the vehicle inertia, $b_{e,m}$ is the lumped viscous damping coefficient at the motor output shaft, T_f can be treated as disturbance, T_m is the output torque of the motor. The right three parts of Equation (2) are known as incline resistance, aerodynamic resistance and rolling resistance. The vehicle inertia is comparatively large and there is no power output during gear shift process, therefore, the vehicle speed ω_v can be assumed to be constant.

As mentioned before, the speed regulation phase is to make ω_m as close as possible to the motor target speed ω_m^T, which can be calculated as:

$$\omega_m^T = \omega_v \cdot i_{m,NG} \tag{3}$$

Where $i_{m,NG}$ is the ratio of the gear to be engaged. It is obviously that the motor speed should decrease to the target speed in gear upshift scenario, the gear downshift process is exactly the opposite. The dynamic characteristics of the motor shaft during the speed synchronization regulation process are mainly determined by Equation (1). Table 1 lists the system parameters for powertrain model.

Table 1: system parameters for powertrain model

Item	Value	Unit
$J_{e,m}$	0.0192	kgm^2
$b_{e,m}$	0.0011	$Nm/(rad/s)$
$i_{m,1}$	27.806	-
$i_{m,3}$	10.318	-
$i_{m,5}$	5.872	-

3 Controller design

The speed regulation phase control can be simplified as a tracking problem, where the reference trajectory can be obtained from Equation (3). Fig. 3 is the block diagram of the combined speed synchronization controller. MPC is adopted to achieve a good tracking performance. It takes the predicted behaviours into accountant so that not only the current tracking error can be suppressed but also the future errors [8]. To enhance the robustness of the nominal controller, a discrete-time DO is added to eliminate effects from external disturbance.

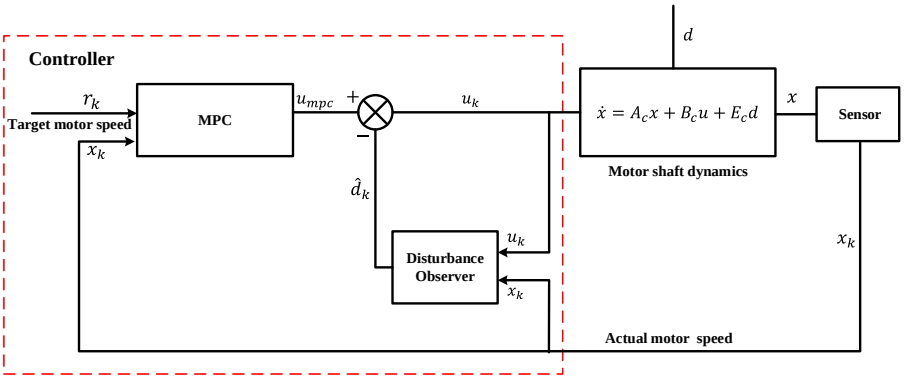

Figure 3: Block diagram of the combined speed synchronization controller

3.1 MPC design

According to Equation (1), the motor shaft dynamics can be represented with the state-space form:

$$\begin{aligned} \dot{x} &= A_c x + B_c u + E_c d \\ \mathrm{y} &= C_c x \end{aligned} \tag{4}$$

Where $x = \omega_m$, $u = T_m$, $A_c = -\frac{b_{e,m}}{J_{e,m}}$, $B_c = E_c = \frac{1}{J_{e,m}}$, $C_c = 1$, and d is the lumped disturbance acting on motor output shaft. Equation (4) can be discretized with a constant sampling time T, which is chosen the same as the sampling period of the speed sensor in real experiment.

$$\begin{aligned} x_{k+1} &= A_d x_k + B_d u_k + E_d d_k \\ \mathrm{y}_k &= C_d x_k \end{aligned} \tag{5}$$

The subscript k is a nonnegative integer denoting the sample number which is connected to time by $t = kT$. Assuming that d is an unknown constant disturbance, it can be removed with incremental modelling technique, where variable is replaced by its difference [9]. The incremental form of the state equation can be derived as follows.

$$\Delta x_{k+1} = A_d \Delta x_k + B_d \Delta u_k \tag{6}$$

Then the augmented model of Equation (5) is:

$$\begin{gathered}\overbrace{\begin{bmatrix}\Delta x_{k+1}\\ y_{k+1}\end{bmatrix}}^{\tilde{x}_{k+1}}=\overbrace{\begin{bmatrix}A_d & 0\\ C_dA_d & 1\end{bmatrix}}^{\tilde{A}}\overbrace{\begin{bmatrix}\Delta x_k\\ y_k\end{bmatrix}}^{\tilde{x}_k}+\overbrace{\begin{bmatrix}B_d\\ C_dB_d\end{bmatrix}}^{\tilde{B}}\Delta u_k\\ \mathrm{y}_k=\overbrace{\begin{bmatrix}0 & 1\end{bmatrix}}^{\tilde{C}}\begin{bmatrix}\Delta x_k\\ y_k\end{bmatrix}\end{gathered} \tag{7}$$

Where the state variable is chosen to be $\tilde{x}_k=\left[\Delta {x_k}^T, y_k\right]^T$.

Let m and p denote control horizon and prediction horizon, respectively. Note that the input variable remains unchanged outside the control horizon. The recursive relation of the state variable can be derived from Equation (7).

$$\tilde{x}_{k+i|k}=\tilde{A}^i\tilde{x}_k+\sum_{l=0}^{i-1}\tilde{A}^l\tilde{B}\Delta u_{k+i-1-l}\ ,\qquad i=1,2,\dots,p \tag{8}$$

Where $\tilde{x}_{k+i|k}$ denotes the predicted state variable at sample instant $k+i$. Since the optimal problem is to adjust the motor speed to target value, the cost of the finite horizon objective can be represented in a standard quadratic form.

$$J=(W-Y)^TQ(W-Y)+\Delta U^TR\Delta U \tag{9}$$

Where W denotes the reference trajectory, Y is the predicted output sequences and can be obtained by substituting Equation (8) into Equation (7). Q is the weighting matrix to penalize track errors, R is related to the control action and can be regarded as a soft constraint imposed on the input variable. In additional, Q is chosen to be real symmetric and positive semidefinite, R is real symmetric and positive definite, W has the structure $W=[1\quad\cdots\quad 1]^Tw_k$ because the target speed is assumed to be constant within the prediction horizon. In order to simplify the analytical process, Q and R are restricted to be diagonal.

Notice that the cost function depends on initial state $\tilde{x}_k$ and input sequences ΔU, then the optimal solution can be formulated as follows.

$$\Delta U^*=\arg\min_{\Delta \mathrm{U}} J(\tilde{x}_k,\Delta U) \tag{10}$$

MPC has the capacity to handle constrained optimal problem, but the output and state constraints are always inactive in speed regulation phase. Based on the convex optimization theory [10], in the absence of constraints, Equation (10) can be solved as:

$$\Delta U^*=\left({S_u}^TQS_u+R\right)^{-1}{S_u}^TQ(W-S_x\tilde{x}_k) \tag{11}$$

The moving horizon control law uses the first move of the optimal control sequence, that is, the optimal control at step k is:

$$\Delta u_k^*=[1\quad\cdots\quad 0]\Delta U^*=K_yw_k-K_x\tilde{x}_k \tag{12}$$

Where

$$K_x=[1\quad\cdots\quad 0]\left({S_u}^TQS_u+R\right)^{-1}{S_u}^TQS_x$$
$$K_y=[1\quad\cdots\quad 0]\left({S_u}^TQS_u+R\right)^{-1}{S_u}^TQ[1\quad\cdots\quad 1]^T$$

Equation (12) gives a feedforward-feedback control law. If the weighting matrices are determined, the gain matrices can be precomputed off-line and the control action applied to the plant can be obtained on-line.

3.2 MPC parameters tuning

Unconstrained MPC is equivalent to unconstrained LQR control with infinite horizon, so it inherits the tuning challenge of the weighting matrices Q and R. According to Equation (11), tuning parameters of the MPC consist of control horizon, prediction horizon and weighting matrices. Each of the above parameters has a specific role in system performance and it is not always obvious to select an appropriate value.

The closed-loop system is given by substituting Equation (12) into Equation (7):

$$\tilde{x}_{k+1} = (\tilde{A} - \tilde{B}K_x)\tilde{x}_k + \tilde{B}K_y w_k \tag{13}$$

Since Equation (13) represents a second-order discrete-time system, a quantitative relationship between the closed-loop performance and tuning parameters can be obtained. The s-plane transfer function of a continuous second-order system is given by:

$$G(s) = \frac{Y(s)}{X(s)} = \frac{\omega_n^2}{s^2 + 2\xi\omega_n s + \omega_n^2} \tag{14}$$

Where ξ is the damping ratio and ω_n is the undamped natural frequency of the system. The step response of Equation (14) can be described by the maximum overshoot δ and the settling time t_s. In our work, a small settling time and overshoot mean a smooth speed regulation process, i.e., a good gear shift quality. In the case of giving the requirements of the settling time and maximum overshoot, the matching transfer function $G(s)$ can be uniquely obtained. Then the desired discrete-time closed-loop pole locations $p_{desired}$ can be given from the corresponding discrete-time equivalent of $G(s)$. The gain matrix K_x in Equation (12), satisfying the specified pole locations $p_{desired}$, can be derived from Ackermann formula [11]. K_y can be directly given by the last columns of the gain matrix K_x due to the specific form of state transition matrix and output matrix in Equation (7), i.e., $K_y = [0 \quad \cdots \quad 1]^T K_x$. Revisiting Equation (12), it can be seen that the gain matrices can be obtained once the weighting matrices are determined, and vice versa. Suppose that the control horizon m is 1, then R is a single-element matrix with a scalar r and Q is a diagonal matrix with the structure $diag(q_1, \cdots, q_p)$.

The above steps give the gain matrices with the specified closed-loop pole locations $p_{desired}$, then Q and R need to satisfy the following equation:

$$\left(S_u{}^T Q S_u + \mathrm{R}\right)^{-1} S_u{}^T Q S_x - K_x = 0 \tag{15}$$

Considering the unknowns r and $q_1, \cdots, q_p$, Equation (15) can be rewritten as:

$$f(r, q_1, \cdots, q_p) = 0 \tag{16}$$

Notice that the equality constraints may be too restrictive to get the solution, it is worthwhile to introduce a relaxation variable α. Hence it can be transformed into a linear programming (LP) problem with inequality constraints.

$$\min_{Q,R,\alpha} \alpha_1 + \alpha_2 \tag{17}$$

Subject. to

$$-\alpha_i \le f_i(r, q_1, \cdots, q_p) \le \alpha_i \qquad i = 1,2$$
$$\mathrm{Q} \succ 0, \mathrm{R} \succcurlyeq 0$$
$$\alpha_i \ge 0$$

There are many general solutions to the above optimization problem, such as interior point method and active set method, etc. For further details of LP problem, refer to Wright's work [10].

3.3 Disturbance observer design

Parameters mismatch and model uncertainty can degenerate control performance, sometimes it may cause unstable and oscillation. The incremental form MPC design can suppress unknown constant disturbance to some extent, but it is useless against random perturbation. To solve the problem, a discrete-time disturbance observer for Equation (5) is introduced as:

$$\begin{cases} \hat{d}_k = Lx_k - z_k \\ z_{k+1} = z_k + L\left(A_d x_k + B_d u_k + E_d \hat{d}_k\right) - Lx_k \end{cases} \tag{18}$$

Where $\hat{d}_k$ is the estimation of the disturbance d, z_k is an intermediate variable, L is the observer gain and can be tuned to satisfy different estimation demands.

Contrary to the hypothesis that the disturbance is constant in MPC design, the disturbance here is assumed to be slowly time-varying in actual speed synchronization circumstance, that is $|\Delta d_k| \le \varepsilon,\ \forall k = 1, \dots, \infty, \varepsilon \in N$.

Disturbance estimate error is defined as $e_{d_k} \triangleq d_k - \hat{d}_k$. From Equation (5) and (18), the recursive relation of the estimate error can be derived as:

$$e_{d_{k+1}} = (I - LE_d)e_{d_k} + \Delta d_{k+1} \tag{19}$$

Equation (19) is asymptotically stable if the eigenvalues of $I - LE_d$ are less than unity, which means the estimate error converges to a bound as T increases.

$$\underbrace{\left|e_{d_{k+n}}\right|}_{n\to\infty} = \lim_{\mathrm{n}\to\infty} \left| (I - LE_d)^n e_{d_k} + \sum_{i=1}^{n-1} (I - LE_d)^{i-1} \Delta d_{k+i} \right| \approx \frac{\varepsilon}{LE_d} \tag{20}$$

Equation (5) is a scalar equation. Hence, the observer gain should satisfy the following equation and the value of L can be tuned for a robustness or aggressive estimate speed.

$$0 \le L \le \frac{2}{E_d} \tag{21}$$

4 Results

4.1 Simulation results and analysis

To validate the effectiveness of the proposed controller, simulations are carried out with a high-fidelity HDCT powertrain model in this section. The motor speed of the 1-3 upshift point n_m is 3058 rpm according to the designed shift schedule, then the target speed is 1135 rpm. To avoid the appearance of "kick tooth" phenomenon and obtain a small initial speed slip at the beginning of gear engagement phase, the acceptable speed synchronization error in 1-3 upshift should be less than 50 rpm from synchronizer bench test results.

The maximum overshoot δ in speed regulation phase is chosen as 15%, and the settling time t_s corresponding to the above speed synchronization error bandwidth is 0.4 s. Then the closed-loop pole locations

are at $P_{desired}$=0.8971±0.1434i. The MPC tuning parameters can be obtained by solving the convex optimization problem defined in Equation (17). Table 2 lists the main parameters for MPC design.

Table 2: MPC parameters used to generate the desired closed-loop poles (at $\alpha \leq$ 1e-4)

N_p	N_c	Q	R
6	1	diag(0.0198,0.0124,0.110,0.0123,0.0192,0.1672)	8.7829

Fig. 4 shows the speed synchronization control process with MPC parameters in Table 2. The result shows that, the maximum overshoot and the settling time are coincide with the desired preset values. Moreover, the motor output torque is relatively small during speed regulation phase. That is a proof why an unconstrained MPC is applied rather than the constrained MPC, because the optimization solutions fall within the feasible domain, i.e., the motor torque control sequences are under the physical limits.

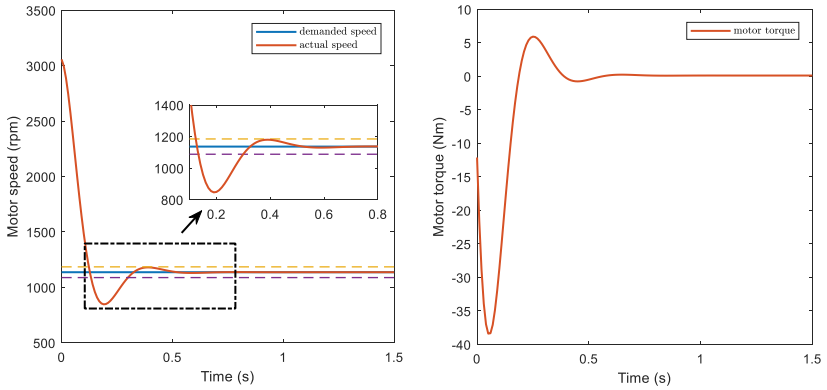

(a) Speed synchronization response (b) Motor torque response

Figure 4: The 1-3 upshift process with the desired poles

The controller performance is subjected to model parameters uncertainty, unmodeled dynamics and measurement noises, etc., where these disturbances are usually difficult to measure and analysis in practice. Hence, in order to verify the robustness of the controller in the presence of disturbances, a hypothetical disturbance is introduced and is assumed as:

$$d(t) = 2\,sin(20\pi t + 1) + 1.5\,cos(4\pi t) + 2.1866 \tag{22}$$

The results of the simulations for speed regulation process with disturbance compensation are shown in Fig. 5. It can be observed that the disturbance observer can reduce the maximum overshoot and suppress speed fluctuation. To illustrate the effects of different observer gains, we set the observer gain L to be 0.5 and 2, respectively. However, since the characteristics of disturbances are unknown, the observer gain L employed here may be no longer suitable for other disturbance circumstances.

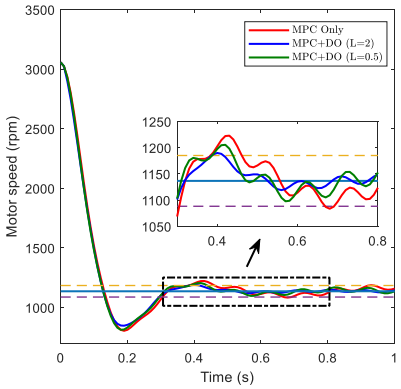

Figure 5: Speed synchronization performances with DO method

4.2 Experiment results and analysis

To demonstrate the effectiveness of the proposed scheme in practice, an experimental platform for the HDCT powertrain system is set up as Fig. 6. It consists of the HDCT gearbox, dynamometers, and flywheel. The dynamometer is connected over the output shaft of the HDCT to apply the load, and the flywheel is to emulate the vehicle inertia. The algorithm is compiled and loaded into MicroAutoBox simulator, which is a real-time digital system. Moreover, the delivery of signals between TCU, PCU and MicroAutoBox simulator is achieved through the CAN bus.

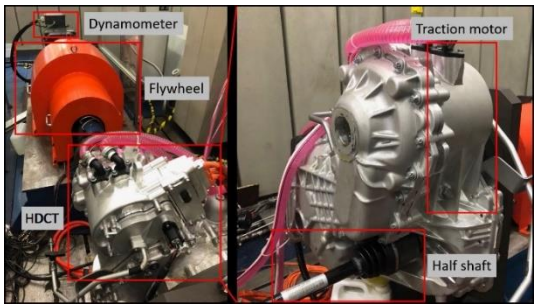

Figure 6: Test bench for the HDCT powertrain system

Fig. 7 shows the test results of a typical 1-3 upshift process. Since the actual disturbance cannot be compensated completely, there are some differences exists between the results of Fig. 7 and that of Fig. 4 in simulation section. However, the maximum overshoot and settling time in experiment are roughly coincided with the preset values. The total gear shift time is about 1.2s, which satisfies the design shift time requirement of the HDCT powertrain system.

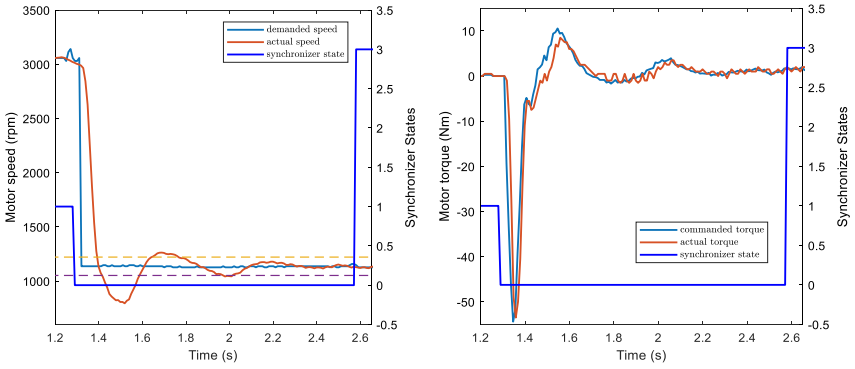

(a) Speed synchronization response (b) Motor torque response

Figure 7: The 1-3 upshift process in experiment (at t_s=0.4s and δ=15%)

To highlight the effectiveness of the proposed algorithm, a PI cascade speed controller is adopted to make a comparation. From Fig. 8, it can be seen that the speed synchronization performance employed the combined controller is better than that by employing the nominal MPC control, where the maximum overshoot is significantly reduced, endorsing the effectiveness of disturbance observer. And we can guess that the actual disturbance is slowly time-varying, because when the motor speed is near the target speed, the speed fluctuation of nominal MPC control is almost the same as that of the combined control. Parameters of the PI controller are chosen based on the Empirical Ziegler-Nichols technique [12]. These two sets of PI controller parameters can both realize 1-3 upshift process. As indicated in subgraph of Fig. 8, a long transient process is unsatisfactory, which results in a large output torque hole of the vehicle. The time of gear change event completed with first PI method is 0.8s behind that of the MPC method. Worse still, if integrating gain is too small, like the second PI controller, it takes nearly two times of the shift time since the static error cannot be eliminated.

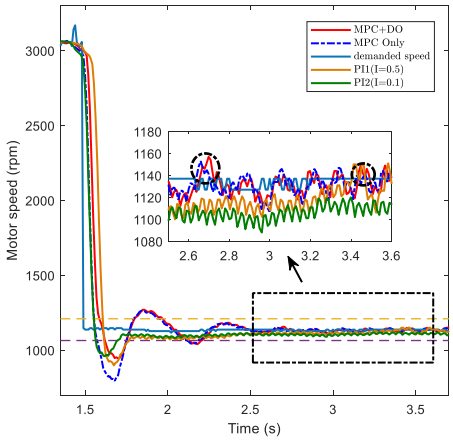

Figure 8: Speed synchronization performance with MPC+DO and PI methods

5 Conclusions

In this work, the speed regulation phase control for a HDCT powertrain in pure electric drive mode is dealt with a robust speed synchronization controller which combines MPC and disturbance observer. Unconstrained MPC is equivalent to unconstrained LQR control with infinite horizon, so it inherits the tuning challenge of the weighting matrices Q and R. The MPC gains obtained with the proposed tuning procedure give a good benchmark for parameters selection in practice. The unknown constant disturbance can be removed by using incremental model, moreover, a discrete-time disturbance observer is used to enhance the robustness of the algorithm. Simulation and experiment results show that the combined control method can realize a fast and robust motor speed regulation process. In addition, the method used in this paper is also applicable to other CLAMT systems in electric and hybrid electric vehicles.

Acknowledgments

The authors would like to thank Chinese National Key Technology R&D Program (Grant No. 2015BAG04B01) for the support on this project.

References

[1] Walker, P., Fang, Y. and Zhang, N. *Dynamics and Control of Clutchless Automated Manual Transmissions for Electric Vehicles*, Journal of Vibration and Acoustics, ISSN 1048-9002, 139(2017), 1-13

[2] Lei, Z., Sun, D., Liu, Y., Qin, D., Zhang, Y., Yang, Y. and Chen, L. *Analysis and coordinated control of mode transition and shifting for a full hybrid electric vehicle based on dual clutch transmissions,* Mechanism and Machine Theory, ISSN 0094-114X, 114(2017), 125-140

[3] Ranogajec, V. and Deur, J. *Bond graph analysis and optimal control of the hybrid dual clutch transmission shift process*, Journal of Multi-body dynamics, ISSN 1464-4193, 231(2017), 480-492

[4] Liu, H., Lei, Y., Li, Z., Zhang, J. and Li, Y. *Gear-Shift Strategy for a clutchless automated manual transmission in battery electric vehicles*, International Journal of Commercial Vehicles, ISSN 1946-391X, 5(2012), 57-62

[5] Yu, C. H. and Tseng, C. Y. *Research on gear-change control technology for the clutchless automatic–manual transmission of an electric vehicle,* Journal of Automobile Engineering, ISSN 0954-4070, 227(2013), 1446-1458

[6] Tseng, C. Y. and Yu, C. H. *Advanced shifting control of synchronizer mechanisms for clutchless automatic manual transmission in an electric vehicle*, Mechanism and Machine Theory, ISSN 0094-114X , 84(2015), 37-56

[7] Zhong, Z., Kong, G., Yu, Z., Xin, X. and Chen, X. *Shifting control of an automated mechanical transmission without using the clutch*, International Journal of Automotive Technology, ISSN 1229-9138, 13(2012), 487–496

[8] Rawlings, J. B. and Mayne, D. Q. *Model Predictive Control: Theory and Design*, ISBN 978-0975937730, Madison, Nob Hill Publishing, 2009

[9] Chai, S., Wang, L. and Rogers, E. *Model predictive control of a permanent magnet synchronous motor with experimental validation,* Control Engineering Practice, ISSN 0967-0061, 21(2013), 1584-1593

[10] Wright, S. and Nocedal, J. *Numerical Optimization,* ISBN 978-0-387-40065-5, New York, Springer Science, 2006

[11] Kautsky, J., Nichols, N. K. and Van Dooren, P. *Robust pole assignment in linear state feedback,* International Journal of control, ISSN 1366-5820, 41(2007), 1129-1155

[12] Meshram, M.P. and Kanojiya, G.R. *Tuning of PID controller using Ziegler-Nichols method for speed control of DC motor,* International Conference On Advances In Engineering, Science and Management, 2012, 117-122

Authors

Wei Huang was born in Anhui, China, in 1993. He received the B.S.degree in vehicle engineering from Xi'an Jiao Tong University, Xi'an, China, in 2014. He is currently working toward the Ph.D. degree with the School of Mechanical Engineering, Shanghai Jiao Tong University, Shanghai, China. His research interests include dynamics and control for advanced powertrain systems.

Jianlong Zhang was born in Henan, China, in 1976. He received the Ph.D. degree in vehicle engineering from Shanghai Jiao Tong University, Shanghai, China, in 2009. He is currently an associate professor of Shanghai Jiao Tong University. His major research interests are powertrain control, coordinated control of electric vehicles and automotive software engineering.

Jianfeng Huang was born in Guangdong, China, in 1989. He is a PhD candidate in Shanghai Jiao Tong University. His research interest includes configuration design, parameter optimization, and gear shift control of different kinds of transmissions for electric vehicles and hybrid electric vehicles.

Chengliang Yin was born in Inner Mongolia, China, in 1965. He received the Master and Ph.D. degree in vehicle engineering from Jilin University, China, in 1996 and 2000, respectively. He is currently a Full Professor of Shanghai Jiao Tong University, where he is also the Vice Director of National Engineering Laboratory for Automotive Electronic Control Technology. His research interests include control of automotive electronics, electric vehicles, especially the research and development of hybrid electric vehicles.

Lifang Wang received her Bachelor, Master and Ph.D. degree from Jilin University, China, in 1992, 1994 and 2007, respectively. She is currently a Full Professor of the Institute of Electrical Engineering of Chinese Academy of Sciences, where she is also the Vice Dean of key Laboratory of power electronics and transmission. Her research interests include electric vehicle control, lithium-ion power battery system, wireless charging and electromagnetic compatibility technology.